Distribution of the O-acetyl groups and β-galactofuranose units in galactoxylomannans of the opportunistic fungus Cryptococcus neoformans

Previato, Jose O.; Vinogradov, Evgeny; Maes, Emmanuel; Fonseca, Leonardo M.; Guerardel, Yann; Oliveira, Priscila A. V.; Mendonça-previato, Lucia

Publisher's version / Version de l'éditeur:
https://doi.org/10.1093/glycob/cww127
Glycobiology, 2016-12-16

Glycobiology Advance Access published December 16, 2016

Distribution of the *O*-acetyl groups and β-galactofuranose units in galactoxylomannans of the opportunistic fungus *Cryptococcus neoformans*

Key words: Cryptococcus/ galactofuranose/ galactoxylomannans/ *O*-acetyl/ Capsular polysaccharides

Jose O. Previato[1], Evgeny Vinogradov[2], Emmanuel Maes[3], Leonardo M. Fonseca[1], Yann Guerardel[3], Priscila A. V. Oliveira[1], Lucia Mendonça-Previato[1,*]

[1]Laboratório de Glicobiologia, Instituto de Biofísica Carlos Chagas Filho, Universidade Federal do Rio de Janeiro, 21941902, Rio de Janeiro, Brasil

[2] National Research Council, 100 Sussex Dr, K1A 0R6 Ottawa, Canada

[3] Univ. Lille, CNRS, UMR 8576, UGSF, Unité de Glycobiologie Structurale et Fonctionnelle, F 59000 Lille, France

* Correspondence should be addressed to L.M-P luciamp@biof.ufrj.br; Tel: +55-21-39386646).

Supplementary data: Supplementary figures 1 to 7 in a 10 page pdf file with the manuscript title and authors' names (supplementary data.pdf)

Abstract

Galactoxylomannans (GalXMs) are a mixture of neutral and acidic capsular polysaccharides produced by the human opportunistic fungus *Cryptococcus neoformans* that exhibit potent suppressive effects on the host immune system. Previous studies describing the chemical structure of *C. neoformans* GalXMs have reported species without *O*-acetyl substituents. Herein we describe that *C. neoformans* grown in capsule-inducing medium produces highly *O*-acetylated GalXMs. The location of the *O*-acetyl groups was determined by NMR spectroscopy. In the neutral GalXM (NGalXM), 80% of 3-linked mannose (α-Man*p*) residues present in side chains are acetylated at the *O*-2 position. In acidic GalXM also termed glucuronoxylomannogalactan (GXMGal), 85% of the 3-linked α-Man*p* residues are acetylated either in the *O*-2 (75 %) or in the *O*-6 (25 %) position, but *O*-acetyl groups are not present at both positions simultaneously. In addition, NMR spectroscopy and methylation analysis showed that β-galactofuranose (β-Gal*f*) units are linked to *O*-2 and *O*-3 positions of non-branched α-galactopyranose (α-Gal*p*) units present in the GalXMs backbone chain. These findings highlight new structural features of *C. neoformans* GalXMs. Among these features, the high degree of *O*-acetylation is of particular interest, since *O*-acetyl group-containing polysaccharides are known to possess a range of immunobiological activities.

Introduction

C. neoformans is an opportunistic fungus that causes a systemic mycosis in immunocompromised individuals, especially those with HIV infection, lymphoproliferative diseases, or immunosuppressive therapy (Mitchell and Perfect 1995; Perfect and Casadevall 2002; Park et al. 2009). The infection is initiated by inhalation of infectious particles of desiccated yeast cells or basidiospores from the environment (Heitman 2011). In healthy individuals, *C. neoformans* can be cleared or can lead to a latent infection in the lungs, but in immunosuppressed individuals it can multiply and disseminate to the brain, inducing meningoencephalitis (Sabiiti and May 2012). *C. neoformans* has several well-defined virulence factors that allow the fungus to evade of host defense mechanisms, such as the presence of a polysaccharide capsule and the production of melanin (Kozel 1995; Gomez and Nosanchuk 2003; Doering 2009). The polysaccharide capsule is a characteristic feature of *C. neoformans* conferring resistance to phagocytosis and oxidative stress (Kozel and Gotschlich 1982; Zaragoza et al. 2008). Moreover, capsular polysaccharides are constantly shed into bodily fluids and tissues during the infection (Bloomfield et al. 1963; Wilson et al. 1968; Eng et al. 1986; Grinsell et al. 2001), giving rise to potent immunosuppressive effects on the host immune system (Vecchiarelli 2000). The *C. neoformans* capsule is composed of glucuronoxylomannan (GXM), galactoxylomannans (GalXMs), alongside a small amount of mannoproteins (Cherniak et al. 1988; Cherniak et al. 1998; Heiss et al. 2009). Most of the structural, biological and genetic studies on the capsular polysaccharides have focused on the GXM, which comprises 88% of the capsule mass and is composed of a α-(1→3)-mannopyranose (Man*p*) backbone modified by β-xylopyranose (Xyl*p*), β-glucopyranosyluronic acid (GlcA*p*) and 6-*O*-acetyl substituents (Bhattacharjee et al. 1984; Cherniak et al. 1988; Cherniak and Sundstrom 1994). Also, the variations in the extent and position of *O*-acetylation and Xyl*p* substitutions on the Man*p* backbone of GXM leads to antigenic variability, which gives rise to the classification of *C. neoformans* strains into five serotypes (A, B, C, D, and A-D) (Belay and Cherniak 1995). In the host, GXM enhances fungus survival by virtue of its potent immunomodulatory properties, such as inhibition of phagocytosis (Bulmer and Sans 1968; Kozel and Mastroianni 1976), apoptosis induction in T-cells and macrophages (Syme et al. 1999; Chiapello et al. 2003), alteration in the cytokine synthesis patterns of leukocytes (Vecchiarelli et al. 1995; Retini et al. 1996; Delfino et al. 1997), and inhibition of leukocyte migration to infectious sites (Dong and Murphy 1995;

Ellerbroek et al. 2004). Several studies also show that glucuronoxylomannogalactan (GXMGal), which comprises 8% of capsule mass, also exhibits potent immunomodulatory properties, with deleterious effects on the host immune system (Vecchiarelli et al. 2011). GXMGal inhibits proliferation of T cells and peripheral blood mononuclear cell (PBMC), increases IFN-γ and IL-10 production, and induces T cell apoptosis mediated by caspase-8 (Pericolini et al. 2006; Pericolini et al. 2009; Pericolini et al. 2010). GXMGal is also able to induce TNF-α expression, iNOS expression and NO production, and FAS/FASL-mediated apoptosis in macrophages (Villena et al. 2008). GXMGal consists of a (1→6)-linked α-galactan backbone, where every second α-Gal*p* residue is substituted at *O*-3 with α-Man*p*-(1-3)-α-Man*p*-(1-4)-β-Gal*p*-β1- side chains, which are in turn substituted with a variable number of β-1,2- and β-1,3-Xyl*p* and β-1,3-GlcA residues (Cherniak et al. 1998; Heiss et al. 2009). Recently, it was found that a variable number of branched α-Gal*p* residues of the GXMGal backbone can be substituted at their *O*-2 position by galactofuranose (Gal*f*) (Heiss et al. 2013). Although the most well studied capsule polysaccharides related to *C. neoformans* virulence are GXM and GXMGal, earlier studies on polysaccharides released in the culture supernatants of the CAP-67 mutant strain showed, besides GXMGal, the presence of a neutral galactoxylomannan (NGalXM) (Vaishnav et al. 1998), whose chemical structure and biological properties have not yet been determined (Vaishnav et al. 1998). During our structural characterization of this capsule polysaccharide we observed in proton NMR spectra strong resonance signals at a chemical shift compatible with *O*-acetyl groups. This finding prompted us to verify if the GXMGal purified concomitantly with the NGalXM could also be *O*-acetylated. Here we show that both GXMGal and NGalXM are highly *O*-acetylated, and we determined the location of *O*-acetyl groups in both *C. neoformans* polysaccharides. In addition, we performed the structural characterization of NGalXM, and revised the location of Gal*f* units on the GXMGal backbone. These findings establish new structural features of the complex and biologically active capsule polysaccharides of *C. neoformans*.

Results

Isolation, purification and composition of NGalXM and GXMGal

The GalXMs recovered from culture supernatant of *C. neoformans* CAP-67 strain by ethanol precipitation and isolated by Con-A affinity chromatography were used for the purification of NGalXM and GXMGal by anion-exchange chromatography. GalXMs were fractionated on a Mono Q column into a minor polysaccharide fraction (NGalXM 9.8%) that was eluted with 10 mM sodium phosphate buffer pH 7.2; and a major polysaccharide fraction (GXMGal 91.2%) that was eluted with 180 mM NaCl in the same buffer (supplementary data Figure S1). Gel-filtration chromatography of both polysaccharides gave a single symmetrical peak with an apparent molecular mass of 45.1 kDa (supplementary data Figure S2). Chemical composition analysis showed that both polysaccharides were similar except by the presence of GlcA units in GXMGal (Table I).

Location of O-acetyl groups in NGalXM and GXMGal

To determine the site(s) of the *O*-acetyl groups, NGalXM and GXMGal were analyzed by a set of 1D and 2D NMR homo and heteronuclear experiments.

For the NGalXM, fifteen monosaccharide spin systems (Figure 1 and Table II) were identified as α-Man*p* (A, A', A", D, D'); α-Gal*p* (B, C, C', M); β-Gal*p* (H); β-Gal*f* (K, L); and xylose (X, X', Y). Whereas for GXMGal, nineteen monosaccharide spin systems (Figure 2 and Table III) were identified as α-Man*p* (A, A', A", A*, D, D', E); α-Gal*p* (B, C, C', M); β-Gal*p* (G, H); β-GlcA*p* (F); β-Gal*f* (K, L); and β-Xyl*p* (X, X', Y) by their characteristic COSY, TOCSY, NOESY and HSQC resonance signals. In addition, *O*-acetyl spin systems were also identified in both NGalXM and GXMGal (Tables II and III and supplementary data Figures S3 and S4). Information on the linkages, monosaccharide sequence of the sugar residues, and location of *O*-acetyl groups was obtained from NOESY, HMBC and HSQC spectra.

The HSQC spectrum (Figure 1 insert, and Table II) of NGalXM showed ^{1}H-^{13}C cross-peaks at 5.03/99.1 (α-Gal-B), 5.01/99.1 (α-Gal-C) and 4.68/105.5 (β-Gal-H) ppm in the anomeric region that are typical of those of the *C. neoformans* GXMGal backbone -6)-α-Gal*p* (C)-(1-6)-α-Gal*p* (B)-(1- substituted at *O*-3 of α-Gal*p* (B) with β-Gal*p* (H) (Heiss et al. 2009; Heiss et al. 2013). Confirmation of the linkages and monosaccharide sequence was obtained from the NOESY spectrum (Figure 3, black) that showed inter-residue nOes between B1:C6 and C1:B6, as well as weak nOes between C1:B4, 5 and

from the HMBC spectrum that showed correlations involving C1:B6, B1:C6, and H1:B3 (data not shown).

The HSQC spectrum (Figure 1 insert) also showed anomeric ^{1}H-^{13}C cross-peaks at 4.52/101.4 (β-Xyl-X), 5.20/102.9 (α-Man-A'), 4.41/104.9 (β-Xyl-Y), 4.99/100.9 (α-Man-D) and 4.68/105.5 (β-Gal-H) ppm. Such cross-peaks are similar to those described for the β-Gal*p* side chains of *C. neoformans* GXMGal, with β-Xyl (X)-(1-3)-α-Man (A')-(1-3)[β-Xyl (Y)-(1-2)-]-α-Man (D)-(1-4)-β-Gal(H) sequence (Heiss et al. 2009; Heiss et al. 2013). However, the ^{1}H-^{13}C cross-peak at 5.20/102.9 ppm that arises from Man-A' residues (Figure 1 insert) is present as a low-intensity signal when compared with that observed in the HSQC spectrum of GXMGal (Heiss et al. 2013). On the other hand, a strong ^{1}H-^{13}C cross-peak (Man A) was observed at 5.26/100.1 ppm, which was assigned to H/C-1 of 2-*O*-acetylated α-Man A'. The 2-*O*-acetyl substitution on Man-A was confirmed by the downfield chemical shift of its H-2 signal to 5.39 ppm, along with inter-residue nOes observed in the NOESY spectrum between H-1 and H-2 of Man (A) with the acetyl methyl protons at 2.18 ppm (supplementary data Figure S5). Furthermore, the HSQC spectrum (Figure 1) showed a cross peak of H2/C-2 of Man (A) at 5.39/70.1 ppm and one *O*-acetyl methyl cross-peak at 2.18/ 21,7 ppm (supplementary data Figure S3 insert).

The monosaccharide sequence of the NGalXM side chain was confirmed by the presence in the NOESY spectrum (Figure 3 black) of inter-residue nOes between X1:A3; Y1:D:1, 2; A1:D3; D1:H4, 6; and corresponding HMBC correlations (data not shown). Therefore, the oligosaccharide-repeating unit of NGalXM without β-Gal*f* residues had the structure shown in Figure 4A. Some heterogeneity was apparent in the NMR spectra due to incomplete *O*-acetylation of Man A, giving origin to the Man A' signal, and incomplete *O*-acetylation and substitution of Man A with Xyl, yielding the A'' signal (Figure 1 insert and Table II). HSQC integration of Man A, A' and A'' anomeric ^{1}H-^{13}C cross-peaks showed that 80 % of the 3-linked Man residues of NGalXM side chains were acetylated at the *O*-2 position and substituted on *O*-3 with xylose (Table IV).

The presence of two spin-systems of β-Gal*f* in the NMR spectra of NGalXM (Figure 1 insert) identical to those previously found in the GXMGal (Heiss et al. 2013), prompted us to revise the location of the β-Gal*f* residues in the *C. neoformans* GalXMs, since it was expected to find just one β-Gal*f* spin system in the absence of GlcA. Initially the

linkage of both β-Gal*f* residues was determined based on nOe data only. First, inter-residue nOes were observed between H-1 of β-Gal*f* (L) and H-1 of minor α-Gal*p* residues designated α-Gal (M) L1:M1 (supplementary data Figure S6), and between the H-1 of β-Gal*f* (L) and the H-2 of α-Gal*p* residues designated α-Gal (M) L1:M2 (Figure 3, black). These two inter-residue nOes confirmed that β-Gal*f* (L) was linked to *O*-2 of α-Gal*p* (M). The H-1 of β-Gal*f* (K) showed an inter-residue nOe with the H-3 of α-Gal*p* (M), K1:M3 (Figure 3, black), thus leading to the structure shown in Figure 4B. This arrangement of β-Gal*f* substituents agrees with the methylation data presented in (Table V). However, the structure proposed here differs from the published one (Heiss et al. 2013), in which all Gal*f* units are placed on the *O*-2 of α-Gal*p* residues of the backbone chain branched at *O*-3 position with β-Gal*p* units (Figure 4C), although two β-Gal*f* spin-systems are always present in the 2D NMR spectra.

To confirm our proposed linkage position for β-Gal*f* residues, we analyzed by NMR a partially purified GalM isolated from *C. neoformans* mutant strain (NE 321), which lacks the UDP-glucose dehydrogenase (Moyrand and Janbon 2004). This mutant is unable to add Xyl and GlcA residues in the capsular polysaccharides.

The NMR spectra (Figure 5A and B) of GalM showed signals corresponding to six hexopyranose and two hexofuranose spin systems related to those found in *C. neoformans* GalXMs, which were identified as α-Man*p* (A, D), α-Gal*p* (B, C, M), β-Gal*p* (H) and β-Gal*f* (K and L), (Table VI). In addition, three resonance signals observed in the NMR spectra (supplementary data Figure S7) designated N, P and F not related to those found GalXMs were assigned as α-Man, α-Man and β-Glc, respectively (Table VI). The main differential characteristics found in the NMR spectra of GalM in comparison to those of NGalXM are a higher intensity in the β-Gal*f* resonance signals, the absence of 2-*O*-acetylated-Man, and Xyl residues (Figures 5 A and B). Thus, inter-residue nOes characteristic of an α(1→6)-linked Gal*p* backbone -6αGal (C)1→6αGal (B)1- substituted at *O*-3 of α-Gal (B) with β-Gal (H) were observed between B1:C6, C1:B6 and H1:B3 (Figure 6 black). β-Gal*p* (H) was substituted at *O*-4 with the α-Man*p* (A)-(1-3)-α-Man*p* (D) sequence, since inter-residue nOes were observed between A1:D3, 4; and D1:H4, 5, 6 (Figure 6 black). The remaining nOes between L1:M2 (β-Gal*f* L to α-Gal M), K1:M3 (β-Gal*f* K to α-Gal M), and M1:B6 (α-Gal M to α-Gal B) confirmed that a variable number of unbranched α-Gal residues in the NGalXM backbone are substituted at the *O*-2 and *O*-3 positions with β-Gal*f* (Figure 6, black). The

same conclusion was drawn from HMBC and HSQC spectra (Figure 7A and B) which showed correlations L1:M2 (β-Gal*f* L to α-Gal M), and K1:M3 (β-Gal*f* K to α-Gal M). Furthermore, the presence of 1-6 linked α-Gal*p* residues di-substituted with two non-reducing end units of Gal*f* was confirmed by the detection of methyl-2,3,5,6-tetra-*O*-methyl-galactofuranoside and methyl-2,3,6-tri-*O*-acetyl-4-mono-*O*-methyl-galactopyranoside in a molar ratio of 1.7 in the methylation analysis (Table V).
The HSQC spectra (Figure 2 and insert) of GXMGal differed from that of NGalXM by a decrease in the intensity of β-Gal*f* resonance signals, along with the presence of additional signals related to the *O*-acetylation state and addition of the terminal β-GlcA*p*. One feature of these spectra was the duplication of the -3→αMan1→4β-Gal signals caused by non-stoichiometric addition of β-GlcA (F) at *O*-3 of β-Gal residues. Thus, four spin systems were observed for α-Man (D and E) and β-Gal (G and H), (Figure 2 insert). Position of the GlcA (F) followed from the observation of a NOESY (red) correlation between F1:G3 (supplementary data Figure S8) and the β-Gal (G) C-3 chemical shift observed at 81.3 ppm, 8 ppm downfield relative to its position in the β-Gal-H residue (Figure 2). The terminal location of GlcA*p* residues was confirmed by the presence of methyl-2,3,4,6-tetra-*O*-methyl-glucoside in the methylation analysis of carboxyl-reduced GXMGal (Table V). The additional *O*-acetyl group was located at C-6 of the α-Man (A*) residues, present in the side chains of GXMGal repeating units. The *O*-6 acetylation of the α-Man-A* residue followed from downfield shift of H-6 split signals to 4.34 and 4.40 ppm and of the C-6 signal to 65.1 ppm from their usual locations around 3.82/62.0 ppm, and the observation of an additional *O*-acetyl signal at 2.19/21.8 ppm in the HSQC spectrum supplementary data Figure S4 insert. Moreover, *O*-6 acetylation was confirmed by the presence of nOe cross-peaks between $-CH_3$ group (δ 2.19) from *O*-acetyl and H1 and H6,6´ of Man A* residue (supplementary data Figure S9). HSQC integration of anomeric ^{1}H-^{13}C cross peaks of Man A, A',A``and A* (Figure 2 insert and Table VII) shows that 85 % of 3-linked Man residues of the GXMGal side chains were acetylated. Also, integration of Man A H-2 and Man A* H-6,6' of ^{1}H-^{13}C cross peaks (Table VII) reveals that *O*-acetylation occurs at either the C-2 (75 %) or the C-6 (25 %), but not at both positions simultaneously. Thus, we propose for the acidic oligosaccharide-repeating unit of the GXMGal the structures depicted in Figure 4D and 4E and for neutral oligosaccharide repeating units, with Gal*f* units, the structure shown in Figure 4F.

Discussion

Previous studies on the GXMGal from *C. neoformans* established the chemical structure of this capsular polysaccharide excluding determination of possible non-carbohydrate substituents such as *O*-acetyl ester. Generally, the GXMGal have a (1-6)-linked alpha-D-Gal*p* backbone substituted in the 3-positions of alternate Gal*p* units by β-Xyl -(1-3)-α-Man*p*-(1-3)[β-Xyl -(1-2)-]-α-Man*p*-(1-4)-β-Gal*p* side chains.

The aforementioned studies were performed on GXMGal isolated from the culture supernatants of *C. neoformans* serotype D CAP 67 strain, grown in the LDM or YPD medium at 30°C (Vaishnav et al. 1998; Heiss et al. 2009; Heiss et al. 2013). In the present study, we reported new structural features for the galactoxylomannans (NGalXM and GXMGal) isolated from culture supernatants of *C. neoformans* serotype D strain grown under same conditions used by Vaishnav et al., (1998). Our NMR results show that the side chains of NGalXM and GXMGal are highly decorated with *O*-acetyl groups, and that the non-branched Gal*p* units present in the backbone of these polysaccharides can be substituted at *O*-2 and *O*-3 positions by Gal*f* residues. This differs from the previous report in which the Gal*f* residues were found to be linked to position *O*-2 of branched gal*p* units of the GXMGal backbone (Heiss et al. 2013). We also observed the presence of *O*-acetyl groups in the side chains of GXMGal isolated from culture supernatant of *C. neoformans* CAP 67 grown in the LDM medium at 37 °C (data not shown). One likely explanation for the absence of *O*-acetyl groups in the side chains of GXMGal proposed by Vaishnav et al., (1998) may be found in the degradation procedures (Smith degradation and acetolysis) used to elucidate the structure of these polysaccharides. Additionally, the lack of *O*-acetyl substituents in the structure of GXMGal deduced by Heiss et al. (2009; 2013) could be due to the difference in the culture medium composition. In agreement with our suggestion, the anomeric region of the HSQC spectrum of GXMGal published by Heiss et al. (2013) contains a weak ^{1}H-^{13}C cross peak that could be attributable to 2-*O*- acetylated Man*p* residues.

Variations in the polysaccharide constitutions depending on the culture condition used is a phenomenon often observed in fungi (Mendonca et al. 1976; McCourtie and Douglas 1981; Okawa et al. 2005; Gates-Hollingsworth and Kozel 2009; Kudoh et al. 2015). For instance, De Jesus et al (2010), showed that differences in sugar composition, serological reactivity and physical-chemical properties can arise between GalXMs preparations from *C. neoformans* grown under different culture conditions.

Thus, our findings suggest that there is a preferential synthesis of highly *O*-acetylated NGalXM and GXMGal when *C. neoformans* is growth in the LDM medium irrespective on the incubation temperature. However, whether this preferential synthesis of *O*-acetylated NGalXM and GXMGal is maintained in both polysaccharides synthesized *in vivo* or under other growth conditions is not known. The biological significance of the *O*-acetyl groups of *C. neoformans* NGalXM and GXMGal remains to be determined. *O*-acetyl groups are common substituents of cryptococcal capsular GXM and play an important role in modulating the host protective immune responses. The higher virulence of *C. gatti* as compared to *C. neoformans* relies on differences in the *O*-acetylation patterns of the capsular GXM (Urai et al. 2015). While *C. neoformans* GXM induces expression of pro-inflammatory cytokines such as TNF-α and IL-6 by dendritic cells, the corresponding polysaccharide from *C. gatti* does not induce significant production of the same cytokines (Urai et al. 2015). In addition, *O*-acetyl groups are the immunodominant epitopes for the recognition of GXM by monoclonal and polyclonal antibodies (Cherniak et al. 1980; Eckert and Kozel 1987; Belay and Cherniak 1995; Kozel et al. 2003) and play a key role in inhibiting neutrophil migration toward chemotactic stimuli (Ellerbroek et al. 2004). Given the bulky nature of *O*-acetyl groups and their positioning on the NGalXM and GXMGal side chains, we suspect that the extent of *O*-acetylation may affect immunoregulatory properties of these polysaccharides. In fact, one important consequence of our results is that experiments involving interactions of NGalXM and GXMGal with the host cell and subsequent immune response must take into account the possible variation in the content of *O*-acetyl groups caused by different culture conditions used to grow *C. neoformans*. Studies are in progress to characterise further the suppressive role of *O*-acetyl groups of NGalXM and GXMGal on the host innate and adaptative immunity that could contribute to the immune-evasion strategies deployed during cryptococcal infection.

Materials and Methods

C. neoformans strains and growth conditions.

Two *C. neoformans* mutant strains were used in this study. The serotype D acapsular mutant CAP67 (Jacobson et al. 1982) was kindly provided by Dr. Robert Cherniak, from the Georgia State University (Atlanta, GA); and the serotype A *ugd1*Δ mutant strain NE 321 (deletion of the fungal *UGD1* gene, encoding UDP-Glc dehydrogenase) (Moyrand and Janbon 2004) was kindly provided by Dr Guilhem Janbon from the Institut Pasteur (Paris, France). Fresh cultures of *C. neoformans* cells grown on yeast extract peptone dextrose (YPD -1% (w/v) yeast extract, 2% (w/v) peptone, 2% (w/v) dextrose with 2% (w/v) agar) on slant tubes were used as inoculum. Transfers were initially made to flasks containing 30 mL of liquid YPD medium; incubation temperature was 30°C for mutant strain CAP-67, and 28°C for mutant strain NE 321, with continuous shaking (100 rpm). After four days, the 30 mL cultures were used as inoculum for 3 L Erlenmeyer flasks containing 1 L of liquid defined medium (LDM): D-glucose 20 g/L, $KH_2PO_4.H_2O$ l.36 g/L, urea l.29 g/L, sodium glutamate l g/L, and $MgSO_4.7\ H_2O$ 0.3 g/L, supplemented with thiamine.HCI, 2 mg/L; biotin, 10 µg/L. (Cherniak et al. 1982). After 5 days at 30°C or 28°C on a rotatory shaker (100 rpm) cells were harvested by centrifugation.

Isolation and purification of Polysaccharides – Neutral Galactoxylomannan (NGalXM), Glucuronoxylomannogalactan (GXMGal) and Galactomannan (GalM)

NGalXM and GXMGal were isolated from culture supernatant of CAP67 mutant by precipitation with ethanol and purified by affinity and anion exchange chromatography as described by Vaishnav et al. (1998). Culture supernatant from mutant strain CAP67 grown as described above was separated from the cells by centrifugation at 1200 *g* for 30 min at 4°C, concentrated by ultrafiltration using a 10 kDa-cut off spiral cartridge (Amicon/Millipore, USA), and submitted to overnight precipitation at 4°C after addition of three volumes of ethanol. The precipitate containing GalXMs and mannoproteins was dissolved in distilled water, filtered through a 0.45 um filter and lyophilized. The freeze-dried mixture of GalXMs and mannoproteins was dissolved in 10 ml of 5 mM sodium acetate buffer pH 5.2, containing 1 mM $CaCl_2$, 1 mM $MgCl_2$, 1 mM $MnCl_2$ and 0.15 M NaCl (Con-A buffer), and applied to a XK-26/40 column packed with 70 mL ConA-Sepharose 4B (GE Healthcare, Sweeden), equilibrated in the same buffer and

connected to an HPLC system (AKTApurifier GE Healthcare, Sweeden), at a flow rate of 0.25ml/min. The column was washed with 5 column volumes (CV) of Con-A buffer to elute the GalXMs. The flow through and washes were collected as fractions of 10 ml and assayed with phenol-sulphuric acid reaction (Dubois et al. 1956). Fractions containing GalXMs were pooled, concentrated, dialyzed against distilled water and lyophilized. In order to purify NGalXM and GXMGal, the freeze-dried GalXMs was dissolved in 5 ml of 10 mM of sodium phosphate buffer, pH 7.2 and applied to a Mono Q HR 16/10 column (GE Healthcare, Sweden), equilibrated in the same buffer, at a flow rate of 4 mL/min. The column was initially washed with 7 CV of 10 mM of sodium phosphate buffer, pH 7.2 to elute the NGalXM; followed by 15 CV of a linear gradient of NaCl ranging from 0 to 0.5 M in the same buffer to elute GXMGal. The column flow was at the rate of 4 ml/min. Fractions of 6 mL were collected and assayed by the phenol-sulphuric acid reaction. The fractions containing NGalXM or GXMGal were pooled, dialyzed against distilled water, and lyophilized. The resulting NGalXM and GXMGal were further purified by size exclusion chromatography on a 1.6 x 100 cm column of Bio-Gel P-30 fine (Bio-Rad Laboratories), and characterized by NMR spectroscopy and methylation analysis.

GalM was isolated from cells of *C. neoformans* mutant strain NE-321 by aqueous phenol extraction as described by Gutierrez et al. (2007), and partially purified by affinity chromatography on a Con-A column. Briefly, fungus cells (200 g wet weight) were extracted three times with 450 mL of 20 mM citrate buffer, pH 7.0 for 90 min at 121°C (Lloyd and Bitoon 1971). The cell debris remaining after the last centrifugation was extracted with 45% (v/v) aqueous phenol at 75 °C for 30 min. The aqueous layer was extensively dialyzed against water, lyophilized, dissolved in water, and applied to a column (2 x 100 cm) of Bio-Gel P-60 fine (Bio-Rad Laboratories). The carbohydrate peak eluting in the void volume was pooled, lyophilized and treated several times with a mixture of chloroform, methanol and water at a 10:10:3 ratio for extraction of glycoinositolphosphorylceramides (GIPCs). The resulting insoluble material was dissolved in ConA buffer, filtered through a 0.45 µm filter and applied to an HR16/10 column (GE Healthcare, Sweden) packed with 20 mL of ConA-Sepharose 4-B (GE Healthcare, Sweden equilibrated with same buffer, at a flow rate of 0.3 mL/min. The column was washed with 6 CV of Con-A buffer, followed by 8 CV of Con-A buffer containing 0.3 M of methyl α-D-mannopyranoside to eluted GalM. The eluted GalM was dialyzed extensively against water and then lyophilized.

Determination of homogeneity and apparent molecular weight of NGalXM and GXGalM

The homogeneity and apparent molecular weight of NGalXM and GXGalM were determinated on a Shimadzu LC-20A HPLC system equipped with a size exclusion column connected to a Shimadzu refractive index detector (RID-10A). Samples of NGalXM or GXGalM were dissolved in a 50 mM sodium phosphate buffer containing 0.3 M NaCl, pH 7.0 and injected into a TSK gel G4000SW Ultrapac column (7.5 mm id. X 600 mm LKB) that was calibrated using Immunoglobulin G (156.000 Da), Bovine serum albumin (67.000 Da), Ovalbumin (43.000 Da), and Trypsin inhibitor (20.100 Da) as molecular weight standards. The column was equilibrated and eluted with 50 mM sodium phosphate buffer containing 0.3 M NaCl, pH 7.0 at flow rate of 1.0 ml/min.

Carbohydrate analysis

NGalXM, GXMGal and GalM samples were methanolysed with 0.5M methanolic HCl for 18 h at 80 ^{0}C, after addition of *myo*-inositol as internal standard. The metanolysates were dried and trimethylsilylated with bis-(trimethylsilyl) trifluoroacetamide/pyridine 1:1 v/v. The trimethylsilylated methyl glycosides were analysed by gas-liquid chromatography (GC) and GC-mass spectrometry (GC-MS). GC analysis was performed on a Shimadzu 2012 Plus-gas chromatograph equipped with a DB-1 fused silica column (30 m x 0.25 mm internal diameter J&W Scientific) using hydrogen as carrier gas. GC-MS was carried out on a Shimadzu 17 A gas chromatograph interfaced to a Shimadzu GCMS-QP5050 mass spectrometer (electron impact 70 eV), equipped with a DB-1 fused silica column (30 mx 0.25 mm internal diameter, J&W Scientific), using helium as a carrier gas. In both analyses, the column temperature was increased from 120 °C to 240 °C at 2 °C/min.

Carboxyl reduction

The GXMGal was carboxyl-reduced according to Fontaine et al (1994). Prior to the methyl esterification, the GXMGal was converted to its protonated form by passage through H^{+} form Dowex 50 x 2 (200-400 mesh) resin and recovered by lyophilization. Protonated GalXMan-B (10 mg) was dissolved in 5 mL of dimethyl sulfoxide, and methyl esterified at 25 °C for 6 h with diazomethane. The methyl esterified GXMGal

was reduced in a 1 M imidazol/HCl buffer (pH 7.0, 2 mL) by the addition of $NaBD_4$ (200 mg). After 6 h at 4 °C, the excess of $NaBD_4$ was destroyed by the addition of glacial acetic acid. The carboxyl-reduced GXMGal (CR-GXMGal) was dialyzed and freeze-dried.

Methylation analysis

NGalXM, GXMGal, CR-GXMGal and GalM were permethylated by the procedure of Ciucanu and Kerek (1984).The permethylated polysaccharides were recovered by chloroform extraction from reaction mixture, to which a saturated aqueous solution of sodium thiosulfate was previously added. The chloroform extracts were washed 6 times with equal volumes of water, and evaporated under a gentle stream of N_2. The methylated polysaccharides were methanolysed with 0.5 M HCl in methanol for 18 h at 80 °C. The methanolysed samples were dried under nitrogen, and acetylated with acetic anhydride-pyridine (9:1, v/v), for 18 h at room temperature. The resulting mixture of acetylated and partially *O*-methylated methyl glycosides was analysed by GC and GC-MS, peaks being identified by comparison of their retention times to those of authentic standards, and by their mass spectra according to Fournet et al., (1981). The GC and GC-MS analyses were performed as described for carbohydrate analysis, except that the column temperature was increased from 110 °C to 220 °C at 2 °C/min.

O-acetyl quantification of NGalXM and GXMGal

O-acetylation of purified NGalXM and GXMGal was measured colorimetrically according to the Hestrin method described in Gudlavalleti et al (2004). Briefly, samples of 400 a 800 µg of polysaccharides (dissolved in 600µl of H20) were incubated with an equal volume of 0.035 M hydroxylamine in 0.75 M NaOH for 10 min at 25 °C, followed by the addition of 1 M of perchloric acid (600µl) and 70 mM ferric perchlorate in 0.5 M perchloric acid (600ul). The pink color resulting from the presence of *O*-acetyl groups was quantified at 500 nm.

NMR spectroscopy

Samples were solubilized in highly enriched deuterated water (99.96% of deuterium atom, Euriso-Top®, St-Aubin, France) and lyophilized and this operation was twice repeated. Acetone was added as internal standard starting from a solution of 2.5 µL of acetone in 10 mL of D_2O (^1H calibrated at 2.225 ppm and ^{13}C at 31.5 ppm).

NMR spectra were recorded in D_2O solutions at 25-40 °C using Bruker AVANCE III 600, 800 or 900 MHz and Varian Inova UNITY 500 MHz spectrometers in the NMR facilities of Centro Nacional de Ressonância Magnética Nuclear, Rio de Janeiro, Brazil; Platform of NMR spectroscopy of University of Lille 1, France and NRC of Ottawa, Canada) with standard 2D pulse programs.

All pulse sequences were taken from Avance or Bruker library of pulse programs and all delays and pulse were optimized for each machine. Spectral widths were 12 ppm and 200 ppm for proton and carbon observations respectively. For TOCSY mixing time 120 ms was used and both ROESY and NOESY spectra were recorded with 300 ms mixing time. Multiplicity-edited ^{1}H-^{13}C HSQC were recorded with 1536 data points in F2 and 256 in F1 with heteronuclear $^{1}J_{C,H}$ constant of 142.8 Hz (CH, CH_3 signals were positive and CH_2 signals were negative). ^{1}H-^{13}C HMBC experiments were recorded with 4096 datapoints in F2 and 256 in F1 with a spectral width of 200 ppm for F1 (^{13}C) and 8 ppm for proton channel (F2). The coupling constant $^{3}J_{C,H}$ was taken at 6.25 Hz in order to optimize delay for evolution of long range couplings. Resolution was kept <2.5 Hz/point in F2 of H-H correlations.

Funding

This work was supported by Fundação de Apoio à Pesquisa do Estado do Rio de Janeiro (FAPERJ), Conselho Nacional de Desenvolvimento Científico e Tecnológico (CNPq) and Coordenação de Aperfeiçoamento de Pessoal de Nível Superior (CAPES).

Acknowledgments

We thank Mrs. Lana Cristina dos Santos Valvano for the technical assistance.

Abbreviations

ConA, Concanavalin A; COSY, Correlation spectroscopy; GalXMs, galactoxylomannas; Gal*f*, Galactofuranose; GalM, galactomannan; Gal*p*, Galactopyranose; GlcA, Glucuronic acid; GXGalM, glucuronoxylomannogalactan; HMBC, Heteronuclear multiple-bond correlation ; HSQC, Heteronuclear single quantum correlation; Man*p*, Mannopyranose; NGalXM, Neutral galactoxylomannan; NOESY, Nuclear Overhauser effect spectroscopy; TOCSY, Total correlation spectroscopy; Xyl*p*, Xylopyranose.

References

Belay T, Cherniak R. 1995. Determination of antigen binding specificities of Cryptococcus neoformans factor sera by enzyme-linked immunosorbent assay. Infect Immun. 63:1810-1819.

Bhattacharjee AK, Bennett JE, Glaudemans CP. 1984. Capsular polysaccharides of Cryptococcus neoformans. Rev Infect Dis. 6:619-624.

Bloomfield N, Gordon MA, Elmendorf DF, Jr. 1963. Detection of Cryptococcus Neoformans Antigen in Body Fluids by Latex Particle Agglutination. Proc Soc Exp Biol Med. 114:64-67.

Bulmer GS, Sans MD. 1968. Cryptococcus neoformans. 3. Inhibition of phagocytosis. J Bacteriol. 95:5-8.

Cherniak R, Jones RG, Reiss E. 1988. Structure determination of Cryptococcus neoformans serotype A-variant glucuronoxylomannan by 13C-n.m.r. spectroscopy. Carbohydr Res. 172:113-138.

Cherniak R, Reiss E, Slodki M, Plattner R, Blumer S. 1980. Structure and antigenic activity of the capsular polysaccharide of Cryptococcus neoformans serotype A. Molecular immunology. 17:1025-1032.

Cherniak R, Reiss E, Turner SH. 1982. A galactoxylomannan antigen of Cryptococcus neoformans serotype A. Carbohydr Res. 103:239-250.

Cherniak R, Sundstrom JB. 1994. Polysaccharide antigens of the capsule of Cryptococcus neoformans. Infect Immun. 62:1507-1512.

Cherniak R, Valafar H, Morris LC, Valafar F. 1998. Cryptococcus neoformans chemotyping by quantitative analysis of 1H nuclear magnetic resonance spectra of glucuronoxylomannans with a computer-simulated artificial neural network. Clin Diagn Lab Immunol. 5:146-159.

Chiapello LS, Aoki MP, Rubinstein HR, Masih DT. 2003. Apoptosis induction by glucuronoxylomannan of Cryptococcus neoformans. Med Mycol. 41:347-353.

Ciucanu I, Kerek F. 1984. Rapid and simultaneous methylation of fatty and hydroxy fatty acids for gas—liquid chromatographic analysis. Journal of Chromatography A. 284:179-185.

De Jesus M, Chow SK, Cordero RJ, Frases S, Casadevall A. 2010. Galactoxylomannans from Cryptococcus neoformans varieties neoformans and grubii are structurally and antigenically variable. Eukaryot Cell. 9:1018-1028.

Delfino D, Cianci L, Lupis E, Celeste A, Petrelli ML, Curro F, Cusumano V, Teti G. 1997. Interleukin-6 production by human monocytes stimulated with Cryptococcus neoformans components. Infect Immun. 65:2454-2456.

Doering TL. 2009. How sweet it is! Cell wall biogenesis and polysaccharide capsule formation in Cryptococcus neoformans. Annu Rev Microbiol. 63:223-247.

Dong ZM, Murphy JW. 1995. Intravascular cryptococcal culture filtrate (CneF) and its major component, glucuronoxylomannan, are potent inhibitors of leukocyte accumulation. Infect Immun. 63:770-778.

Dubois M, Gilles KA, Hamilton JK, Rebers P, Smith F. 1956. Colorimetric method for determination of sugars and related substances. Analytical chemistry. 28:350-356.

Eckert TF, Kozel TR. 1987. Production and characterization of monoclonal antibodies specific for Cryptococcus neoformans capsular polysaccharide. Infect Immun. 55:1895-1899.

Ellerbroek PM, Lefeber DJ, van Veghel R, Scharringa J, Brouwer E, Gerwig GJ, Janbon G, Hoepelman AI, Coenjaerts FE. 2004. O-acetylation of cryptococcal capsular glucuronoxylomannan is essential for interference with neutrophil migration. J Immunol. 173:7513-7520.

Eng RH, Bishburg E, Smith SM, Kapila R. 1986. Cryptococcal infections in patients with acquired immune deficiency syndrome. Am J Med. 81:19-23.

Fontaine T, Fournet B, Karamanos Y. 1994. A new procedure for the reduction of uronic acid containing polysaccharides. Journal of microbiological methods. 20:149-157.

Fournet B, Strecker G, Leroy Y, Montreuil J. 1981. Gas--liquid chromatography and mass spectrometry of methylated and acetylated methyl glycosides. Application to the structural analysis of glycoprotein glycans. Anal Biochem. 116:489-502.

Gates-Hollingsworth MA, Kozel TR. 2009. Phenotypic heterogeneity in expression of epitopes in the Cryptococcus neoformans capsule. Mol Microbiol. 74:126-138.

Gomez BL, Nosanchuk JD. 2003. Melanin and fungi. Curr Opin Infect Dis. 16:91-96.

Grinsell M, Weinhold LC, Cutler JE, Han Y, Kozel TR. 2001. In vivo clearance of glucuronoxylomannan, the major capsular polysaccharide of Cryptococcus neoformans: a critical role for tissue macrophages. J Infect Dis. 184:479-487.

Gudlavalleti SK, Datta AK, Tzeng YL, Noble C, Carlson RW, Stephens DS. 2004. The Neisseria meningitidis serogroup A capsular polysaccharide O-3 and O-4 acetyltransferase. J Biol Chem. 279:42765-42773.

Gutierrez AL, Farage L, Melo MN, Mohana-Borges RS, Guerardel Y, Coddeville B, Wieruszeski JM, Mendonca-Previato L, Previato JO. 2007. Characterization of glycoinositolphosphoryl ceramide structure mutant strains of Cryptococcus neoformans. Glycobiology. 17:1-11C.

Heiss C, Klutts JS, Wang Z, Doering TL, Azadi P. 2009. The structure of Cryptococcus neoformans galactoxylomannan contains beta-D-glucuronic acid. Carbohydr Res. 344:915-920.

Heiss C, Skowyra ML, Liu H, Klutts JS, Wang Z, Williams M, Srikanta D, Beverley SM, Azadi P, Doering TL. 2013. Unusual galactofuranose modification of a capsule polysaccharide in the pathogenic yeast Cryptococcus neoformans. J Biol Chem. 288:10994-11003.

Heitman J. 2011. Microbial Pathogens in the Fungal Kingdom. Fungal Biol Rev. 25:48-60.

Jacobson ES, Ayers DJ, Harrell AC, Nicholas CC. 1982. Genetic and phenotypic characterization of capsule mutants of Cryptococcus neoformans. J Bacteriol. 150:1292-1296.

Kozel TR. 1995. Virulence factors of Cryptococcus neoformans. Trends Microbiol. 3:295-299.

Kozel TR, Gotschlich EC. 1982. The capsule of cryptococcus neoformans passively inhibits phagocytosis of the yeast by macrophages. J Immunol. 129:1675-1680.

Kozel TR, Levitz SM, Dromer F, Gates MA, Thorkildson P, Janbon G. 2003. Antigenic and biological characteristics of mutant strains of Cryptococcus neoformans lacking capsular O acetylation or xylosyl side chains. Infect Immun. 71:2868-2875.

Kozel TR, Mastroianni RP. 1976. Inhibition of phagocytosis by cryptococcal polysaccharide: dissociation of the attachment and ingestion phases of phagocytosis. Infect Immun. 14:62-67.

Kudoh A, Okawa Y, Shibata N. 2015. Significant structural change in both O- and N-linked carbohydrate moieties of the antigenic galactomannan from Aspergillus fumigatus grown under different culture conditions. Glycobiology. 25:74-87.

Lloyd KO, Bitoon MA. 1971. Isolation and purification of a peptido-rhamnomannan from the yeast form of Sporothrix schenckii. Structural and immunochemical studies. The Journal of Immunology. 107:663-671.

McCourtie J, Douglas LJ. 1981. Relationship between cell surface composition of Candida albicans and adherence to acrylic after growth on different carbon sources. Infect Immun. 32:1234-1241.

Mendonca L, Gorin PA, Lloyd KO, Travassos LR. 1976. Polymorphism of Sporothrix schenckii surface polysaccharides as a function of morphological differentiation. Biochemistry. 15:2423-2431.

Mitchell TG, Perfect JR. 1995. Cryptococcosis in the era of AIDS--100 years after the discovery of Cryptococcus neoformans. Clin Microbiol Rev. 8:515-548.

Moyrand F, Janbon G. 2004. UGD1, encoding the Cryptococcus neoformans UDP-glucose dehydrogenase, is essential for growth at 37 degrees C and for capsule biosynthesis. Eukaryot Cell. 3:1601-1608.

Okawa Y, Miyauchi M, Goto K, Giummelly P. 2005. Antigenicity of cell wall mannans of Candida albicans NIH A-207 strain cells cultured in galactose-added yeast nitrogen base medium. Biol Pharm Bull. 28:391-393.

Park BJ, Wannemuehler KA, Marston BJ, Govender N, Pappas PG, Chiller TM. 2009. Estimation of the current global burden of cryptococcal meningitis among persons living with HIV/AIDS. AIDS. 23:525-530.

Perfect JR, Casadevall A. 2002. Cryptococcosis. Infect Dis Clin North Am. 16:837-874, v-vi.

Pericolini E, Cenci E, Monari C, De Jesus M, Bistoni F, Casadevall A, Vecchiarelli A. 2006. Cryptococcus neoformans capsular polysaccharide component galactoxylomannan induces apoptosis of human T-cells through activation of caspase-8. Cell Microbiol. 8:267-275.

Pericolini E, Gabrielli E, Bistoni G, Cenci E, Perito S, Chow SK, Riuzzi F, Donato R, Casadevall A, Vecchiarelli A. 2010. Role of CD45 signaling pathway in galactoxylomannan-induced T cell damage. PLoS One. 5:e12720.

Pericolini E, Gabrielli E, Cenci E, De Jesus M, Bistoni F, Casadevall A, Vecchiarelli A. 2009. Involvement of glycoreceptors in galactoxylomannan-induced T cell death. J Immunol. 182:6003-6010.

Retini C, Vecchiarelli A, Monari C, Tascini C, Bistoni F, Kozel TR. 1996. Capsular polysaccharide of Cryptococcus neoformans induces proinflammatory cytokine release by human neutrophils. Infect Immun. 64:2897-2903.

Sabiiti W, May RC. 2012. Mechanisms of infection by the human fungal pathogen Cryptococcus neoformans. Future Microbiol. 7:1297-1313.

Syme RM, Bruno TF, Kozel TR, Mody CH. 1999. The capsule of Cryptococcus neoformans reduces T-lymphocyte proliferation by reducing phagocytosis, which can be restored with anticapsular antibody. Infect Immun. 67:4620-4627.

Urai M, Kaneko Y, Ueno K, Okubo Y, Aizawa T, Fukazawa H, Sugita T, Ohno H, Shibuya K, Kinjo Y*, et al.* 2015. Evasion of Innate Immune Responses by the Highly Virulent Cryptococcus gattii by Altering Capsule Glucuronoxylomannan Structure. Front Cell Infect Microbiol. 5:101.

Vaishnav VV, Bacon BE, O'Neill M, Cherniak R. 1998. Structural characterization of the galactoxylomannan of Cryptococcus neoformans Cap67. Carbohydr Res. 306:315-330.

Vecchiarelli A. 2000. Immunoregulation by capsular components of Cryptococcus neoformans. Med Mycol. 38:407-417.

Vecchiarelli A, Pericolini E, Gabrielli E, Chow SK, Bistoni F, Cenci E, Casadevall A. 2011. Cryptococcus neoformans galactoxylomannan is a potent negative immunomodulator, inspiring new approaches in anti-inflammatory immunotherapy. Immunotherapy. 3:997-1005.

Vecchiarelli A, Retini C, Pietrella D, Monari C, Tascini C, Beccari T, Kozel TR. 1995. Downregulation by cryptococcal polysaccharide of tumor necrosis factor alpha and interleukin-1 beta secretion from human monocytes. Infect Immun. 63:2919-2923.

Villena SN, Pinheiro RO, Pinheiro CS, Nunes MP, Takiya CM, DosReis GA, Previato JO, Mendonca-Previato L, Freire-de-Lima CG. 2008. Capsular polysaccharides galactoxylomannan and glucuronoxylomannan from Cryptococcus neoformans induce macrophage apoptosis mediated by Fas ligand. Cell Microbiol. 10:1274-1285.

Wilson DE, Bennett JE, Bailey JW. 1968. Serologic grouping of Cryptococcus neoformans. Proc Soc Exp Biol Med. 127:820-823.

Zaragoza O, Chrisman CJ, Castelli MV, Frases S, Cuenca-Estrella M, Rodriguez-Tudela JL, Casadevall A. 2008. Capsule enlargement in Cryptococcus neoformans confers resistance to oxidative stress suggesting a mechanism for intracellular survival. Cell Microbiol. 10:2043-2057.

FIGURE LEGENDS

Fig. 1: ^{1}H-^{13}C HSQC spectrum of the NGalXM from *C. neoformans* (CH black, CH_2 red). Insert shows anomeric signals. Signal marked with * correlates with a methyl signal only. The cross peaks are labelled as mentioned in the text and in Table II.

Fig. 2: ^{1}H-^{13}C HSQC spectrum of GXMGal from *C. neoformans* (CH black, CH_2 green). Insert shows anomeric signals. Labelled cross peaks in the carbon ring region belong to β-GlcA (F) , β-Gal (G) and α-Man6Ac (A*6) residues. These cross peaks are absent in N-GalXM. Unlabeled cross peaks are present in both GalXMs.

Fig. 3: Overlap of parts of 2D spectra: COSY (green), TOCSY (red) and NOESY (black) of NGalXM from *C. neoformans*. The cross peaks are labelled as mentioned in the text and in Table II.

Fig. 4: Proposed structures of *C. neoformans* GalXMs: **(A)** NGalXM oligosaccharide repeating unit without β-Gal*f*; **(B)** NGalXM oligosaccharide repeating unit with β-Gal*f*; **(C)** acidic oligosaccharide-repeating unit of GXMGal proposed by Heiss et al 2013; **(D**, **E** and **F)** acidic and neutral oligosaccharide-repeating units of GXMGal proposed in this article.

Fig. 5: ^{1}H-^{13}C HSQC spectrum of GalM from *C. neoformans* mutant strain NE 321 (CH black, CH_2 green). **(A)** Anomeric region; **(B)** Ring carbon region. Resonance signals of less intensity are not visible in the spectrum due to the intensity cutoff. The cross peaks are labelled as in Table IV.

Fig. 6: Overlap of parts of the COSY (blue), TOCSY (red), and NOESY (black) spectra of GalM from *C. neoformans* mutant strain NE321. The cross-peaks are labelled as they are mentioned in the text.

Fig. 7: ^{1}H-^{13}C HMBC **(A)** and ^{1}H-^{13}C HSQC **(B)** spectra of GalM from *C. neoformans* mutant strain NE321 mutant giving the heteronuclear vicinal connections between K and L residues on carbons 3 and 2 respectively of residue M. Dashed arrows indicated routing throughout the interesting residues, plain arrows indicated the corresponding carbons.

Table I. Monosaccharide composition analysis of *C. neoformans* NGalXM, GXMGal and GalM

	Mol %		
Sugar[a]	**NGalXM**	**GXMGal**	**GalM**
Xylose	19.8	19.6	-
Mannose	24.6	23.3	35.3
Galactose	46.7	43.3	60.5
Glucose	-	-	4.2
Glucuronic acid[b]	-	4.5	-
O-Acetyl group[c]	8.9	9.3	-

[a] – Identified and quantified by GC

[b] – Determined as glucose after carboxyl reduction of GXMGal.

[c] – Determined by Hestrin method

Table II. ^{1}H and ^{13}C NMR chemical shifts (ppm) of NGalXM from *C. neoformans*

Label	Sugar	H-1	H-2	H-3	H-4	H-5	H-6	C-1	C-2	C-3	C-4	C-5	C-6	*O*-acetyl methyl
A	α-Man*p(2-OAc)*	5.26	5.39	4.25	3.86	3.99	3.82/3.95	100.1	70.1	76.4	66.3	74.5	62.0	2.18/ 21.7
A'	α-Man*p No Ac*	5.20	4.26	4.05	3.79	3.97	3.82/3.95	102.9	68.8	79.2	66.2	74.5	62.0	
A"	α-Man*p No Ac no Xyl*	5.16	4.09	4.05	3.87	3.96	3.82/3.95	103.6	71.2	70.6	67.2	74.5	62.0	

D	α-Man*p*	4.99	4.14	4.09	3.91	4.09	3.94/3.87	100.9	79.8	76.5	67.4	74.4	61.3
D'	α-Man*p No Xyl*	4.99	4.17	4.09	3.91	4.09	3.84/3.87	101.0	79.6	76.5	67.4	74.4	61.3
B	α-Gal*p*	5.03	4.06	4.03	4.31	4.22	3.72/3.94	99.1	68.6	81.2	70.3	70.0	67.9
C	α-Gal*p*	5.01	3.86	3.90	4.04	4.26	3.70/3.96	99.1	69.5	70.6	70.7	70.0	67.7
C'	α-Gal*p*	4.99	3.86	3.77	3.91	4.26	3.70/3.96	99.4	69.5	70.7	70.7	70.0	67.7
H	β-Gal*p*	4.68	3.64	3.77	4.10	3.87	3.75/3.75	105.5	72.2	73.3	78.5	75.9	61.6
X	β-Xyl*p*	4.52	3.29	3.47	3.66	3.36/4.02	-	101.4	73.8	76.7	70.4	66.3	-
X'	β-Xyl*p No Ac*	4.55	3.38	3.50	3.69	3.36/4.02	-	102.1	74.0	76.7	70.4	66.3	-
Y	β-Xyl*p*	4.41	3.32	3.47	3.65	3.32/4.05	-	104.9	73.9	76.8	70.4	66.2	-
M	α-Gal*p*	5.07	3.99	4.03	4.19	-	-	99.2	75.9	77.3	70.3	-	-
K	β-Gal*f*	5.22	4.21	4.08	4.07	3.86	3.69/3.73	110.3	82.6	78.2	84.2	71.8	63.8
L	β-Gal*f*	5.17	4.19	4.08	4.01	3.86	3.69/3.73	110.3	82.7	78.2	83.2	71.8	63.8

Table III. ^{1}H and ^{13}C NMR chemical shifts (ppm) of GXMGal from *C. neoformans*.

Label	Sugar	H-1	H-2	H-3	H-4	H-5	H-6	C-1	C-2	C-3	C-4	C-5	C-6	*O*-acetyl methyl
A	α-Man*p(2-OAc)*	5.26	5.39	4.25	3.86	3.99	3.82/3.95	100.1	70.1	76.4	66.3	74.5	62.0	2.18/ 21.7
A'	α-Man*p No Ac*	5.20	4.26	4.05	3.79	3.97	3.82/3.95	102.9	68.6	79.2	66.2	74.5	62.0	
A"	α-Man*p No Ac no Xyl*	5.16	4.09	4.05	3.87	3.96	3.82/3.95	103.6	71.2	70.6	67.2	74.5	62.0	
*A**	α-Man*p(6-OAc)*	5.14	4.09	3.90	3.74	4.00	4.34/4.40	103.8	71.9	71.8	66.3	72.5	65.1	2.19/ 21.8
D	α-Man*p*	4.99	4.14	4.09	3.91	4.09	3.94/3.87	100.9	79.8	76.5	67.4	74.4	61.3	
D'	α-Man*p No Xyl*	4.99	4.17	4.09	3.91	4.09	3.84/3.87	101.0	79.6	76.5	67.4	74.4	61.3	
E	α-Man*p*	5.12	4.14	4.09	3.91	4.09	3.84/3.87	100.4	79.8	76.5	67.4	74.4	61.3	

B	α-Gal*p*	5.03	4.06	4.03	4.31	4.22	3.72/3.94	99.1	68.6	81.2	70.3	70.0	67.9
C	α-Gal*p*	5.01	3.86	3.90	4.04	4.26	3.70/3.96	99.1	69.5	70.6	70.7	70.0	67.7
C'	α-Gal*p*	4.99	3.86	3.77	3.91	4.26	3.70/3.96	99.4	69.5	70.7	70.7	70.0	67.7
G	β-Gal*p*	4.70	3.77	3.91	4.34	3.82	3.75/3.75	105.8	73.3	81.3	77.5	75.9	61.2
H	β-Gal*p*	4.68	3.64	3.77	4.10	3.87	3.75/3.75	105.5	72.2	73.3	77.5	75.9	61.6
F	β-GlcA	4.71	3.35	3.54	3.57	3.73	-	105.4	74.7	76.7	72.8	76.7	-
X	β-Xyl*p*	4.52	3.29	3.47	3.66	3.36/4.02	-	101.4	73.8	76.7	70.4	66.3	-
X'	β-Xyl*p No Ac*	4.55	3.38	3.50	3.69	3.36/4.02	-	102.1	74.0	76.7	70.4	66.3	-
Y	β-Xyl*p*	4.41	3.32	3.47	3.65	3.32/4.05	-	104.9	73.9	76.8	70.4	66.2	-
M	α-Gal*p*	5.07	3.99	4.03	4.19	-	-	99.2	76.3	-	70.3	-	-
K	β-Gal*f*	5.22	4.21	4.08	4.07	3.86	3.69/3.73	110.	82.6	78.2	84.2	71.8	63.8

								3					
L	β-Gal*f*	5.17	4.19	4.08	4.01	3.86	3.69/3.73	110.3	82.7	78.2	83.2	71.8	63.8

Table IV. Integration of ^{1}H-^{13}C signals of residues A, A' and A'' in order to evaluate the ratio 2-*O*-acetylated mannosyl in NGalXMan of *C. neoformans*

Protons	H1-A	H1-A'	H1-A''
Chemical shifts	5.26	5.20	5.16
Integration value	**1.00**	**0.20**	**0.08**
Sum	**1.28**		

Table V. Methylation analysis of NGalXM, GXMGal, CR- GXMGal and GalM of *C. neoformans*

Compound	Mol %			
	NGalXM	**GXMGal**	**CR- GXMGal**	**GalM**
Methyl 2,3,4 -tri-*O*-methylxylopyranoside	17.3	17.1	16.3	-
Methyl 2,3,4,6-tetra-*O*-methyl mannopyranoside	1.9	3.1	2.8	11.8
Methyl 2,3,4,6-tetra-*O*-methylglucopyranoside	-	-	3.0	-
Methyl 2,3,5,6-tetra- *O*-methylgalactofuranoside	2.8	1.7	1.6	12.9
Methyl 2,3,4,6-tetra-*O*-methyl galactopyranoside	0.2	0.2	0.3	1.2
Methyl 3,4,6 –tri-*O*-methyl-2- *O*-acetylmannopyranoside	0.5	-	-	2.8
Methyl 2,3,6-tri-*O*-methyl-4- *O*-acetylgalactopyranoside	10.9	10.2	10.1	11.7
Methyl 2,4,6-tri-*O*-methyl-3- *O*-acetylmannopyranoside	11.4	11.3	11.4	15.1
Methyl 2,3,4-tri-*O*-methyl-6- *O*-acetylglucopyranoside	0.2	-	-	3.3
Methyl 2,3,4-tri-*O*-methyl-6- *O*-acetylgalactopyranoside	21.6	21.1	20.1	16.9
Methyl 4,6 –di-*O*-methyl-2,3-di-*O*-acetylmannopyranoside	15.5	14.8	14.2	-
Methyl 2,4- di-*O*-methyl-3.6-di- *O*-acetylgalactopyranoside	16.1	15.8	15.5	16.8
Methyl 2,6-di-*O*-methyl-3,4- di-*O*-acetylgalactopyranoside	-	3.8	3.7	-

Methyl 4- mono-*O*-methyl-2,3,6 tri-*O*-acetylgalactopyranoside	1.6	1.1	1.0	7.5

Table VI. ^{1}H and ^{13}C NMR chemical shifts (ppm) of GalM from *C. neoformans*

Label	Sugar	H-1	H-2	H-3	H-4	H-5	H-6	C-1	C-2	C-3	C-4	C-5	C-6
A	α-Man*p*	5.16	4.09	3.91	3.67	3.82	3.75/3.93	103.7	71.6	71.8	68.4	74.8	62.6
D	α-Man*p*	4.88	4.19	3.98	3.85	4.09	3.82/3.82	103.0	71.1	79.8	67.2	74.7	62.1
N	α-Man*p*	5.29	4.07	3.94	3.65	3.76	3.76/3.88	101.8	71.4	71.3	68.1	74.4	62.1
H	β-Gal*p*	4.67	3.62	3.76	4.05	3.79	3.73/3.73	106.1	72.2	73.3	78.7	76.1	61.5
B	α-Gal*p*	5.02	4.04	4.02	4.30	4.22	3.68/3.93	99.1	68.6	81.4	70.5	70.0	67.6
C	α-Gal*p*	4.98	3.84	3.89	4.03	4.22	3.68/3.93	99.3	69.6	71.0	70.7	70.0	67.6
M	α-Gal*p*	5.06	3.97	4.02	4.27	-	-	99.4	76.1	77.6	71.0	-	-
K	β-Gal*f*	5.22	4.18	4.06	4.05	3.85	3.67/3.71	110.4	82.8	78.3	84.1	71.6	63.9
L	β-Gal*f*	5.16	4.19	4.06	3.99	3.85	3.67/3.71	110.5	82.8	78.3	83.7	71.6	63.9
F	β-Glc*p*	4.53	3.33	3.50	3.47	3.63	4.24/3.86	104.3	74.2	76.7	70.7	76.1	-

P	Man*p*	5.04	-	-	-	-	-	103.5	-	-	-	-	-

Table VII. Integration values from ^{1}H-^{13}C HSQC signal of the terminal mannosyl residue of side chains for GXMGal from *C. neoformans*

Protons	H1-A	H1-A'	H1-A''	H1-A*	H2 of 2-O-acetylated Man	H6,6' of 6-O-acetylated Man
Chemical shifts	5.26	5.20	5.16	5.14	5.39	4.34/4.40
Integration value	**0.72**	**0.24**	**0.30**	**0.15**	**1.00**	**0.42**
sum	**1.41**				***1.21**	

*Integration value for H6,6' must be divided by two because two protons contribute to the signal.

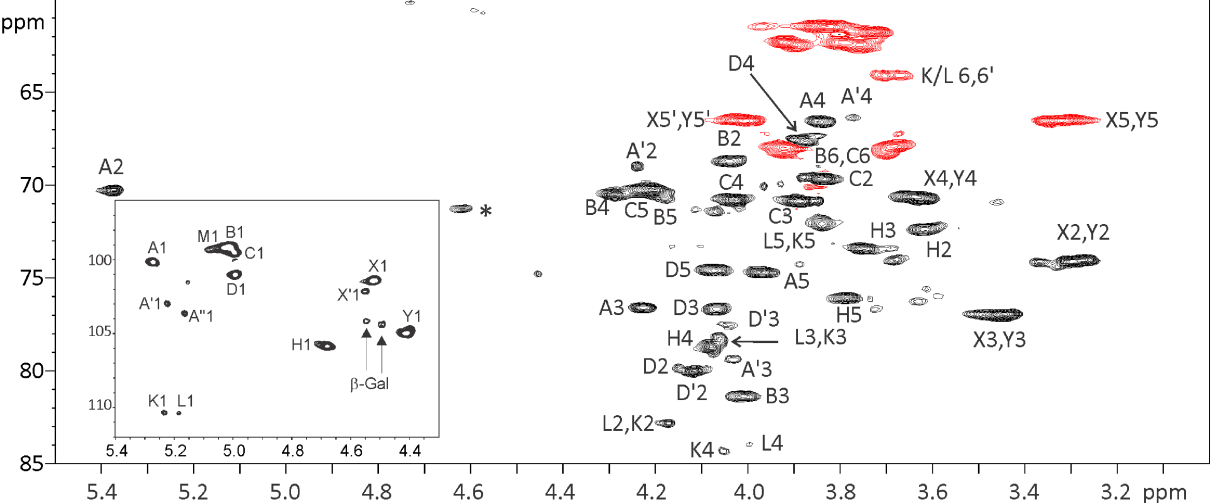
ppm
65
70
75
80
85
5.4
5.2
5.0
4.8
4.6
4.4
4.2
4.0
3.8
3.6
3.4
3.2 ppm
A2
*
D4
K/L 6,6'
A4
A'4
X5',Y5'
X5,Y5
B2
A'2
B6,C6
C4
C2
X4,Y4
B4
C5
B5
C3
L5,K5
H3
H2
X2,Y2
D5
A5
A3
D3
D'3
H5
H4
L3,K3
X3,Y3
D2
A'3
D'2
B3
L2,K2
K4
L4
M1
B1
A1
C1
D1
X1
X'1
A'1
A"1
Y1
H1
β-Gal
K1
L1
100
105
110

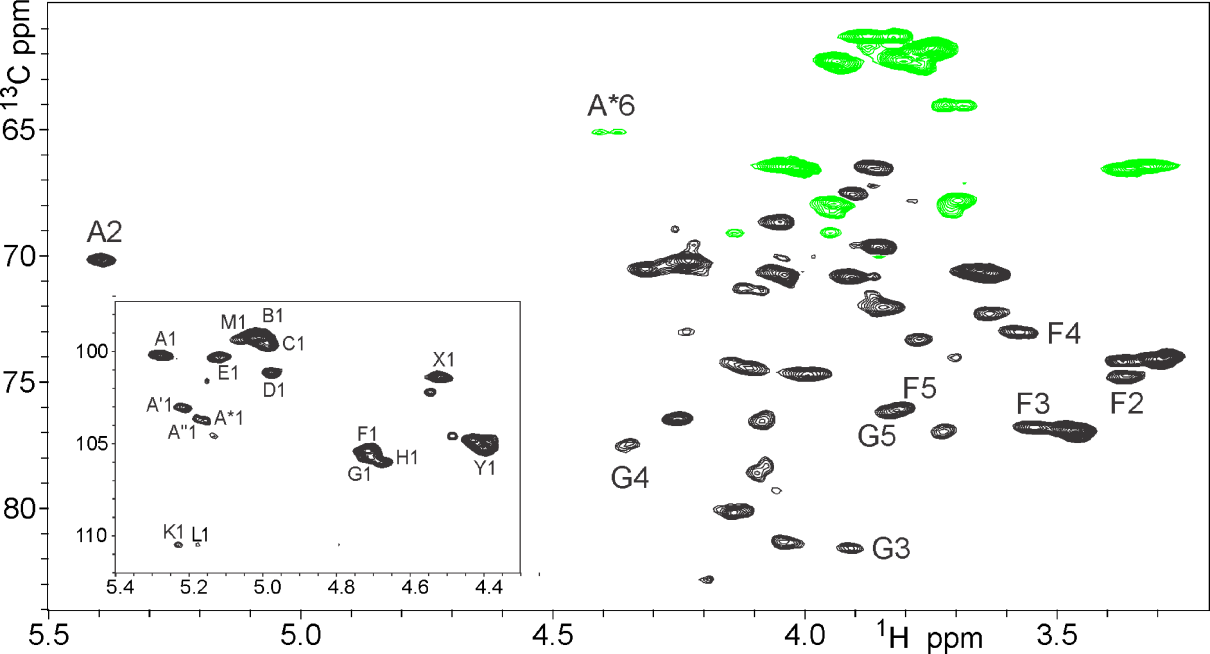
^{13}C ppm
65
70
75
80
A*6
A2
F4
F5
F3
F2
G5
G4
G3
^{1}H ppm
5.5
5.0
4.5
4.0
3.5
A1
M1
B1
C1
E1
D1
X1
A'1
A"1
A*1
F1
G1
H1
Y1
K1
L1
100
105
110
5.4
5.2
5.0
4.8
4.6
4.4

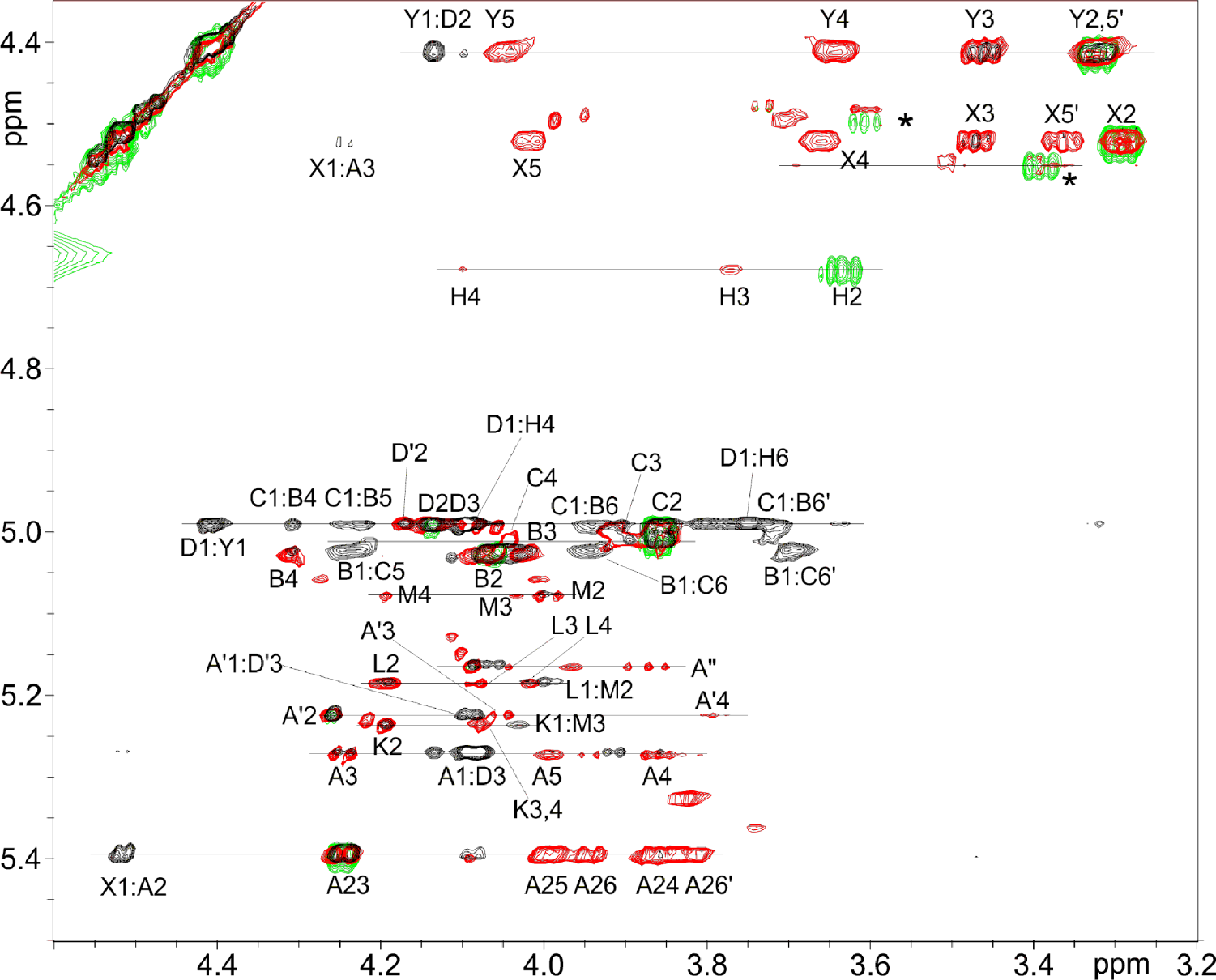
Y1:D2
Y5
Y4
Y3
Y2,5'
X1:A3
X5
X4
X3
X5'
X2
*
*
H4
H3
H2
D1:H4
D'2
C3
D1:H6
C4
C1:B4
C1:B5
D2D3
C1:B6
C2
C1:B6'
B3
D1:Y1
B4
B1:C5
B2
B1:C6
B1:C6'
M4
M3
M2
A'3
L3 L4
A'1:D'3
L2
A"
L1:M2
A'4
A'2
K1:M3
K2
A3
A1:D3
A5
A4
K3,4
X1:A2
A23
A25 A26
A24 A26'
4.4
4.6
4.8
5.0
5.2
5.4
ppm
4.4
4.2
4.0
3.8
3.6
3.4
ppm
3.2

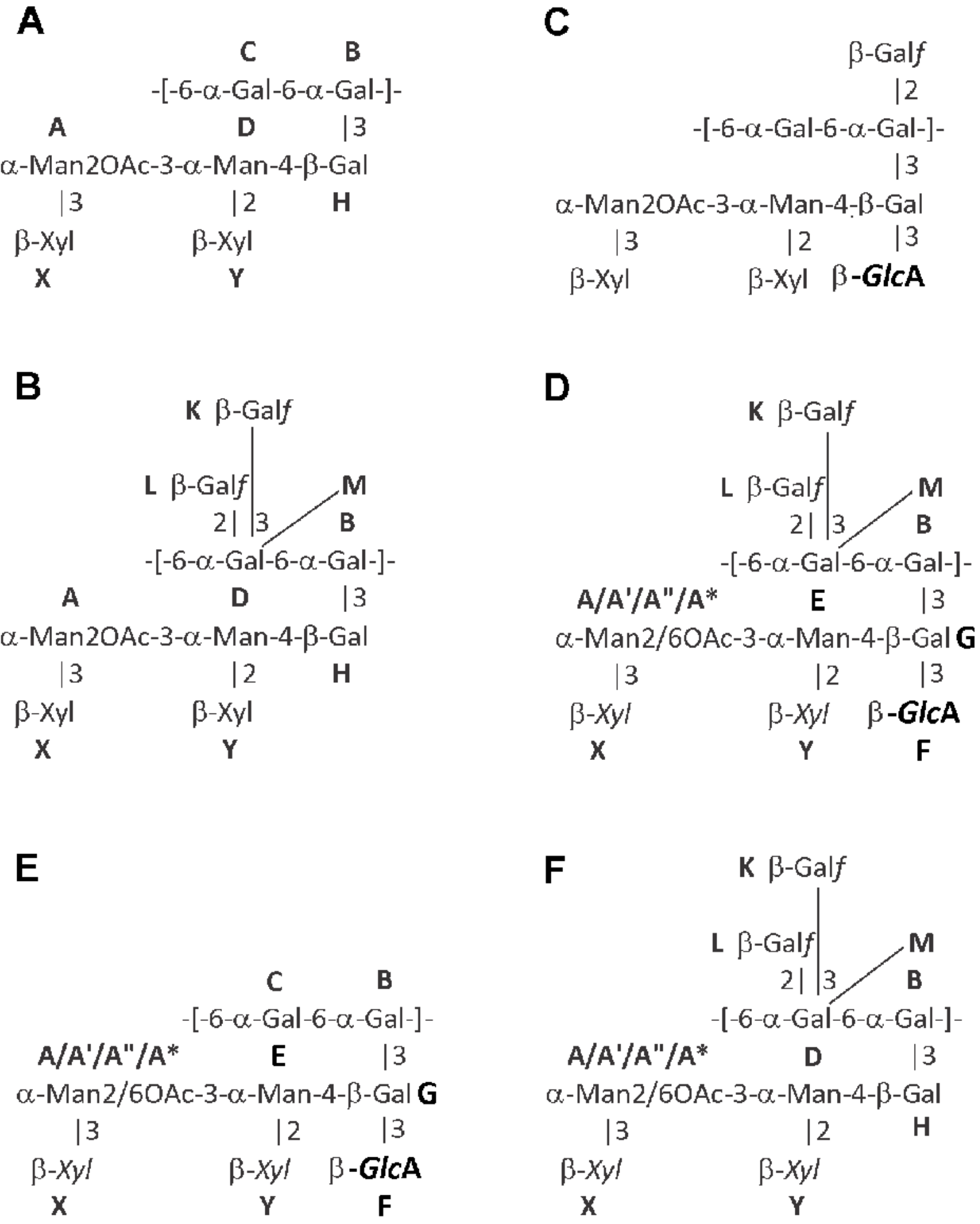
A
C B
-[-6-α-Gal-6-α-Gal-]-
A D |3
α-Man2OAc-3-α-Man-4-β-Gal
|3 |2 H
β-Xyl β-Xyl
X Y
C
β-Gal*f*
|2
-[-6-α-Gal-6-α-Gal-]-
|3
α-Man2OAc-3-α-Man-4-β-Gal
|3 |2 |3
β-Xyl β-Xyl β-**GlcA**
B
K β-Gal*f*
L β-Gal*f* M
2| |3 B
-[-6-α-Gal-6-α-Gal-]-
A D |3
α-Man2OAc-3-α-Man-4-β-Gal
|3 |2 H
β-Xyl β-Xyl
X Y
D
K β-Gal*f*
L β-Gal*f* M
2| |3 B
-[-6-α-Gal-6-α-Gal-]-
A/A'/A"/A* E |3
α-Man2/6OAc-3-α-Man-4-β-Gal G
|3 |2 |3
β-*Xyl* β-*Xyl* β-**GlcA**
X Y F
E
C B
-[-6-α-Gal-6-α-Gal-]-
A/A'/A"/A* E |3
α-Man2/6OAc-3-α-Man-4-β-Gal G
|3 |2 |3
β-*Xyl* β-*Xyl* β-**GlcA**
X Y F
F
K β-Gal*f*
L β-Gal*f* M
2| |3 B
-[-6-α-Gal-6-α-Gal-]-
A/A'/A"/A* D |3
α-Man2/6OAc-3-α-Man-4-β-Gal
|3 |2 H
β-*Xyl* β-*Xyl*
X Y

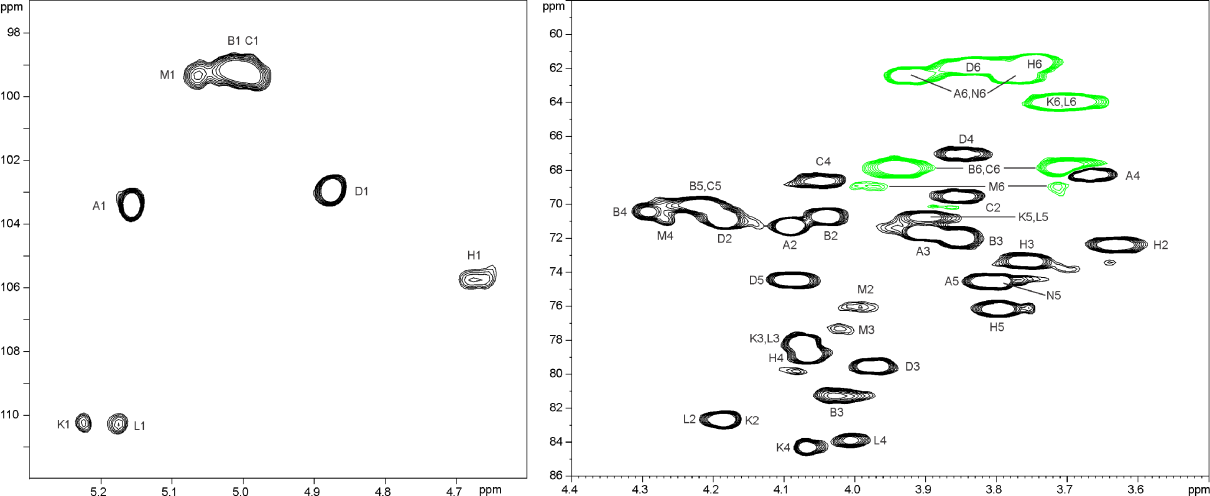
ppm
98
100
102
104
106
108
110
B1 C1
M1
A1
D1
H1
K1
L1
5.2
5.1
5.0
4.9
4.8
4.7
ppm
ppm
60
62
64
66
68
70
72
74
76
78
80
82
84
86
D6
H6
A6,N6
K6,L6
D4
C4
B6,C6
A4
M6
B5,C5
B4
C2
K5,L5
M4
D2
A2
B2
A3
B3
H3
H2
D5
M2
A5
N5
M3
H5
K3,L3
H4
D3
B3
L2
K2
K4
L4
4.4
4.3
4.2
4.1
4.0
3.9
3.8
3.7
3.6
ppm

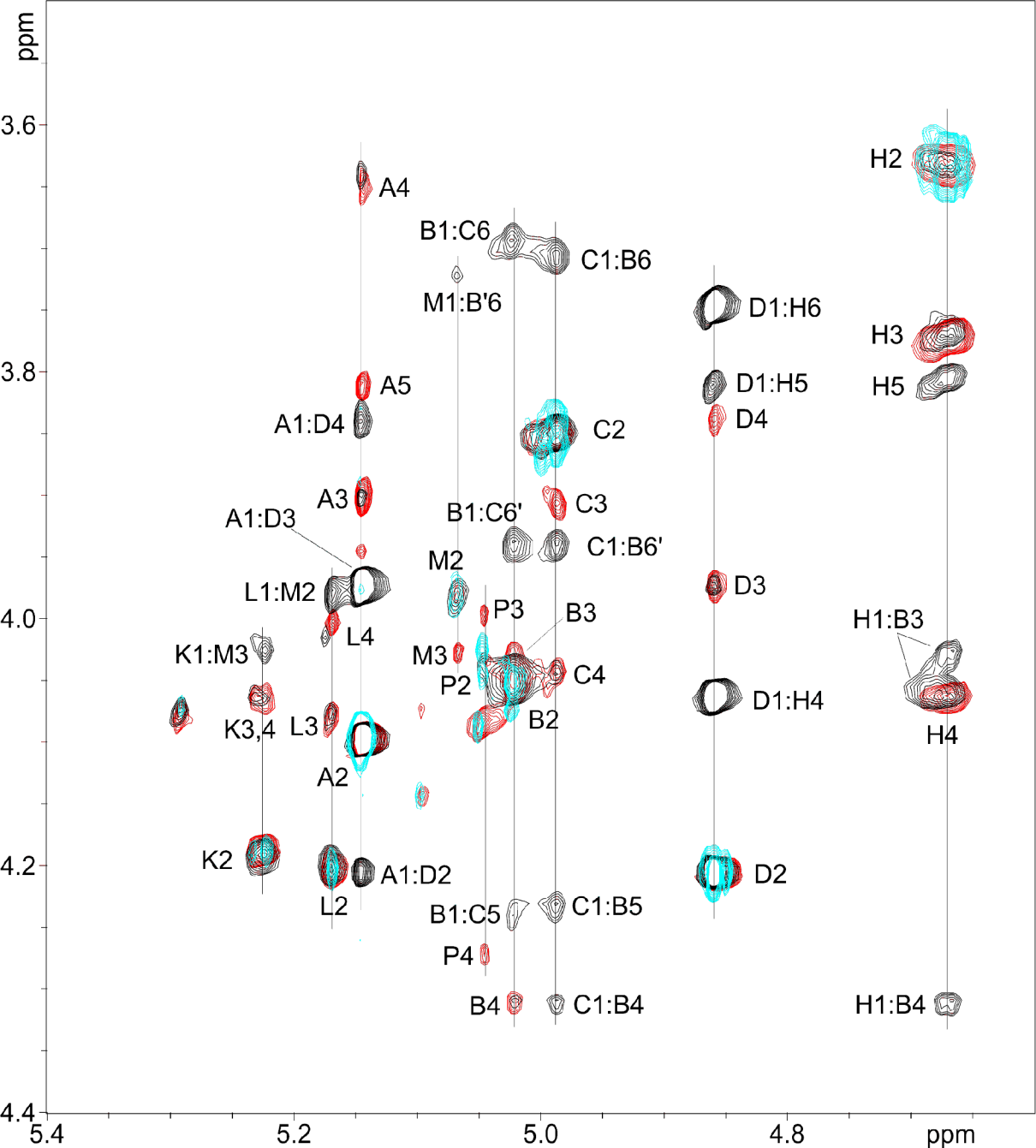
ppm
3.6
3.8
4.0
4.2
4.4
5.4
5.2
5.0
4.8
ppm
A4
B1:C6
C1:B6
M1:B'6
A5
A1:D4
C2
A3
A1:D3
B1:C6'
C3
C1:B6'
M2
L1:M2
P3
B3
L4
K1:M3
M3
P2
C4
K3,4
L3
B2
A2
K2
A1:D2
L2
B1:C5
C1:B5
P4
B4
C1:B4
D1:H6
D1:H5
D4
D3
D1:H4
D2
H2
H3
H5
H1:B3
H4
H1:B4

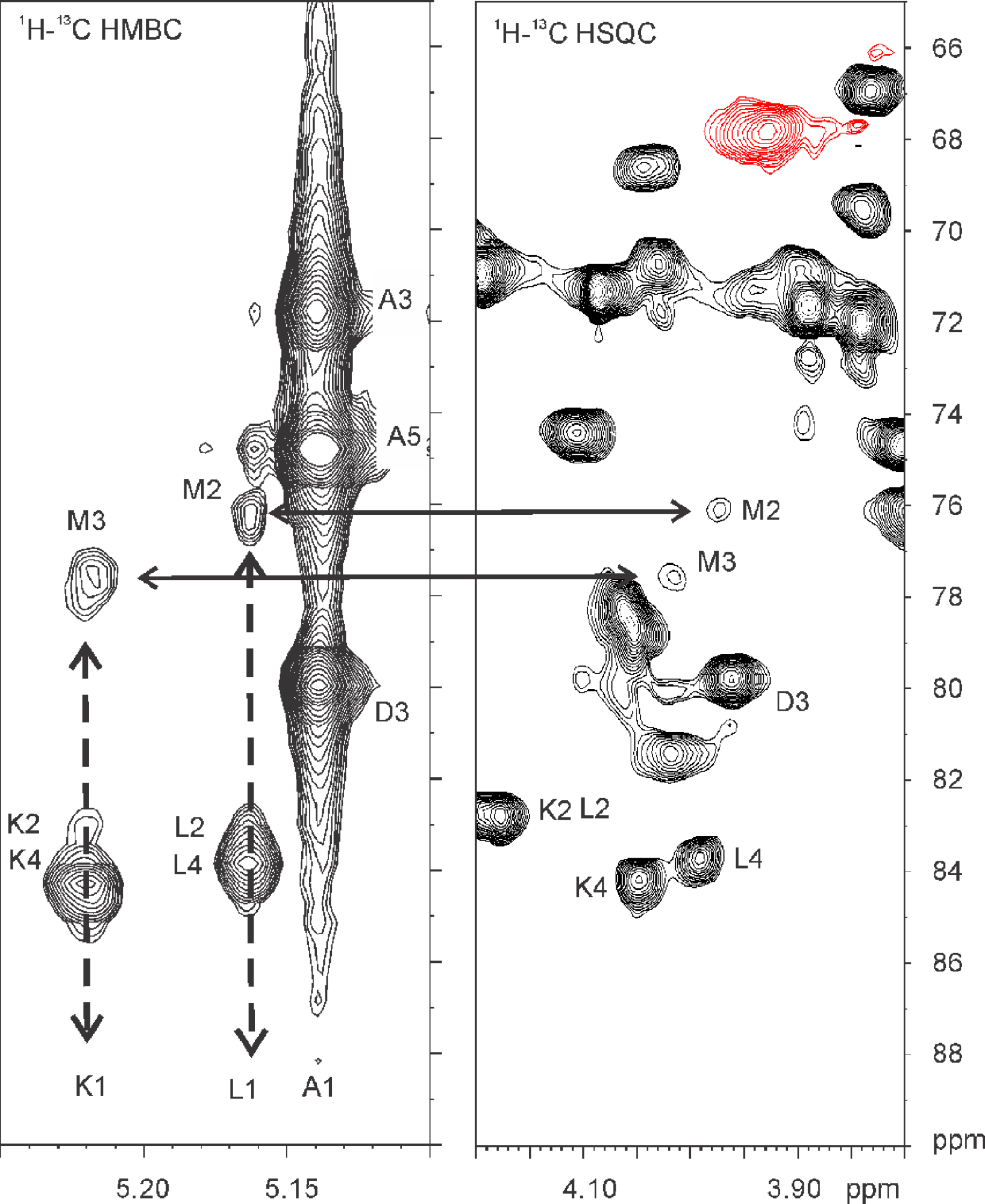
^{1}H-^{13}C HMBC
^{1}H-^{13}C HSQC
A3
A5
M2
M3
D3
K2
K4
L2
L4
K1
L1
A1
M2
M3
D3
K2 L2
L4
K4
66
68
70
72
74
76
78
80
82
84
86
88
ppm
5.20
5.15
4.10
3.90
ppm